

Evaluation of Feature Extraction Techniques for Robust Watermarking

Hae-Yeoun Lee¹, In Koo Kang¹, Heung-Kyu Lee¹, and Young-Ho Suh²

¹ Department of EECS, Korea Advanced Institute of Science and Technology,
Guseong-dong, Yuseong-gu, Daejeon, Republic of Korea
hytoiy@casaturn.kaist.ac.kr

² Digital Content Research Division, Electronics and Telecommunications Research Institute
Guseong-dong, Yuseong-gu, Daejeon, Republic of Korea

Abstract. This paper addresses feature extraction techniques for robust watermarking. Geometric distortion attacks desynchronize the location of the inserted watermark and hence prevent watermark detection. Watermark synchronization, which is a process of finding the location for watermark insertion and detection, is crucial to design robust watermarking. One solution is to use image features. This paper reviews feature extraction techniques that have been used in feature-based watermarking: the Harris corner detector and the Mexican Hat wavelet scale interaction method. We also evaluate the scale-invariant keypoint extractor in comparison with other techniques in aspect of watermarking. After feature extraction, the set of triangles is generated by Delaunay tessellation. These triangles are the location for watermark insertion and detection. Redetection ratio of triangles is evaluated against geometric distortion attacks as well as signal processing attacks. Experimental results show that the scale-invariant keypoint extractor is appropriate for robust watermarking.

1 Introduction

Digital technologies have grown over the last decades, wherein all kinds of multimedia such as image, video, and audio have been digitalized. However, digital multimedia can be copied, manipulated, and reproduced illegally without any quality degradation and protection.

Digital watermarking is an efficient solution for copyright protection of multimedia, which inserts copyright information into contents itself. This information is used as evidence of ownership. Digital watermarking has many applications, in which robustness has been an important issue. There have been many watermarking researches inspired by methods of image coding and compression. Most previous algorithms perform well against signal processing attacks. Nevertheless, in blind watermarking, these algorithms show severe weakness to geometric distortion attacks that desynchronize the location of the inserted copyright information and prevent watermark detection.

In order to resist geometric distortion attacks, watermark synchronization, a process for finding the location for watermark insertion and detection, should be per-

formed. Through this paper, we call this location *the patch*. There have been several solutions for watermark synchronization. The use of periodical sequences [1], the insertion of templates [2], and the use of invariant transforms [3, 4, 5, 6] have been reported among others. One solution to synchronize the watermark location is to use image features. Generally, image features represent an invariant reference for geometric distortion attacks so that referring features can solve watermark synchronization problems.

Kutter *et al.* [7] describe a feature-based synchronization method. First, they extract feature points using a scale interaction technique based on 2D continuous wavelet. Then, they use these points to segment the image, using a Voronoi diagram partitioning of the image. These segments are used as the patches for watermarking. Bas *et al.* [8] extract feature points by applying the Harris corner detector and then decompose the feature points into a set of disjoint triangles by Delaunay tessellation. These triangles are used as the patches for watermarking. Nikolaidis and Pitas [9] describe an image-segmentation based synchronization method. By applying an adaptive k-mean clustering technique, they segment images and select several of the largest regions. The bounding rectangles of these regions are used as the patches for watermarking. Tang and Hang [10] extract feature points using the Mexican Hat wavelet scale interaction method. Disks of fixed radius R , whose centers is the feature points are normalized, because objects in the normalized image are invariant to image distortions. The normalized disks are used as the patches for watermarking.

In watermark synchronization by reference to image features, feature extraction is important for achieving robustness of the watermark. This paper reviews feature extraction techniques that have been used in feature-based watermarking: the Harris corner detector and the Mexican Hat wavelet scale interaction method. We also evaluate an affine-invariant feature extractor called as the scale-invariant keypoint extractor in comparison with other techniques. It is important to redetect the patches in attacked images, which have been detected in the original image for robust watermarking, so we measure redetection ratio of the patches against geometric distortion attacks as well as signal processing attacks. Results show that the scale-invariant keypoint extractor is useful and robust against attacks.

The following section reviews feature extraction techniques and describes the scale-invariant keypoint extractor. Section 3 explains the way to synchronize the location of the watermark. Evaluation results are shown in Section 4. Section 5 concludes this paper.

2 Feature Extraction Techniques

There have been many feature extraction techniques in image processing and computer vision applications. Bas *et al.* [8] compared major feature extraction techniques that consider image gradients: the Harris corner detector, the SUSAN detector, and the Achard-Rouquet detector. The Harris corner detector performed well against image attacks. However, they just focus on the redetection of each feature point, not the patches for watermarking. Image segmentation is commonly used for feature extraction, because segmented regions are expected to be invariant to image distortions. However, the number of regions depends on image contents and its texture. More-

over, their location is sensitive to image distortions [9]. In our opinions, regions from image segmentation are not useful for watermarking purpose. The Mexican Hat wavelet scale interaction method is an intensity-based feature extraction technique and has been used for robust watermarking [7, 10]. In this section, we review two feature extraction techniques: the Harris corner detector and the Mexican Hat wavelet scale interaction method and then describe the scale-invariant keypoint extractor.

2.1 Harris Corner Detector

The Harris corner detector is initially developed for 3D reconstruction [8] and uses image gradients. This detector calculates locally averaged moment matrix computed from image gradients and then combines eigenvalues of the moment matrix to compute a corner-strength, whose local maximums indicate corner locations.

The locally averaged moment matrix $E_{x,y}$ is expressed by

$$E_{x,y} = (x, y)H(x, y)^T \text{ with } H = \begin{bmatrix} D_{x,x} & D_{x,y} \\ D_{x,y} & D_{y,y} \end{bmatrix}. \tag{1}$$

$E_{x,y}$ can be considered as a local auto-correlation function with a shape factor H . D represents image gradient of x - and y -axis. The corner-strength R_H is acquired by combining the eigenvalues as follows.

$$R_H = Det(H) - kTr^2(M), \text{ where } Tr(H) = D_{xx} + D_{yy}, Det(H) = D_{xx}D_{yy} - D_{xy}^2. \tag{2}$$

k is an arbitrary constant. An example of the corner-strength is shown in Fig. 1. Corner points are extracted by searching local maximums on this corner-strength R_H . The Harris corner detector shows high accuracy in corner locations. However, the set of corner points is sensitive to image noise.

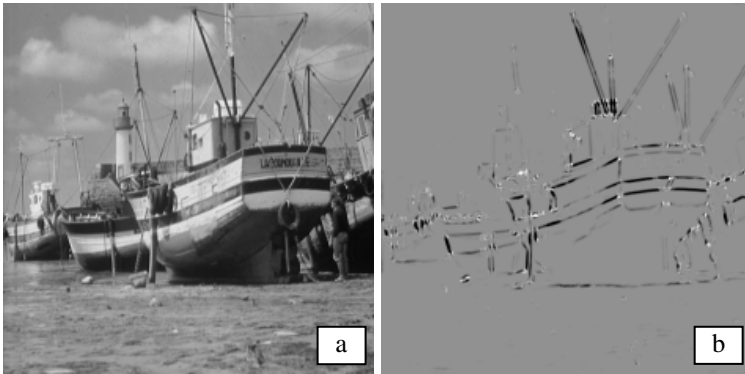


Fig. 1. (a) original image and (b) corner-strength R_H

2.2 Mexican Hat Wavelet Scale Interaction

The Mexican Hat wavelet scale interaction method is initially used in Manjunath *et al.* [11]. Feature points are determined by identifying significant intensity changes

that occur at different scaled version of the same image. This method applies two different scale of the Mexican Hat wavelet to the same image and calculates a scale interaction image between two scaled images. Local maximums of the scale interaction image indicate feature points. The Mexican Hat wavelet, called as Marr wavelet, is invariant to rotation because it has a circularly symmetric frequency response.

The Mexican Hat wavelet at location x is defined as

$$\varphi(\vec{x}) = (2 - |\vec{x}|^2) e^{-|\vec{x}|^2 / 2} \text{ with } |\vec{x}| = (x^2 + y^2)^{1/2}. \quad (3)$$

The 2D Fourier transform of $\varphi(\vec{x})$ is given as follows.

$$\varphi(\vec{k}) = (\vec{k} \cdot \vec{k}) e^{-|\vec{k}|^2 / 2}, \quad (4)$$

where \vec{k} represents 2D spatial frequency.

The scale interaction image is acquired by the following quantities.

$$P_{ij}(\vec{x}) = \left| M_i(\vec{x}) - \gamma \cdot M_j(\vec{x}) \right|, \quad (5)$$

$M_i(\vec{x})$ represents response of the Mexican Hat wavelet at the image location \vec{x} for scale i and j respectively. γ is a normalizing constant. $P_{ij}(\vec{x})$ is the scale interaction between two different scale i and j . Local maximums of $P_{ij}(\vec{x})$ are determined as the set of potential feature points and the points whose strength exceed a threshold are used as the feature points. Fig. 2b and 2c show images filtered by the Mexican Hat wavelet operator with different scale. Fig. 2d shows the scale interaction image between two filtered images and their local maximums are feature points.

2.3 Scale-Invariant Keypoint Extractor

In object recognition and image retrieval applications, affine-invariant features have been recently researched [12, 13, 14]. These features are highly distinctive and matched with high probability against a large case of image distortions, such as view-point changes, illumination condition changes, partial visibility, and image noise. In watermark synchronization using image features, the robustness of features is related to that of watermarking systems. We introduce an affine-invariant feature extractor called as the scale-invariant keypoint extractor [12].

The scale-invariant keypoint extractor considers local image characteristics and retrieves feature points with properties of each point such as the location, the scale, and the orientation. These feature points are invariant to image rotation, scaling, translation, partly illumination changes, and projective transform.

The scale-invariant keypoint extractor detects feature points through a staged filtering approach that identifies stable points in the scale-space. To generate a scale-space, we use a difference of Gaussian function, in which we successively smooth an image with a variable scale (σ_1 , σ_2 , and σ_3) Gaussian filter and calculate difference images by subtracting two successive smoothed images. In this scale-space, we retrieve all local maximums and minimums by checking 8 closest neighborhoods in the same scale and 9 neighborhoods in the scale above and below (see Fig. 3). These locations are invariant to the scale change of images.

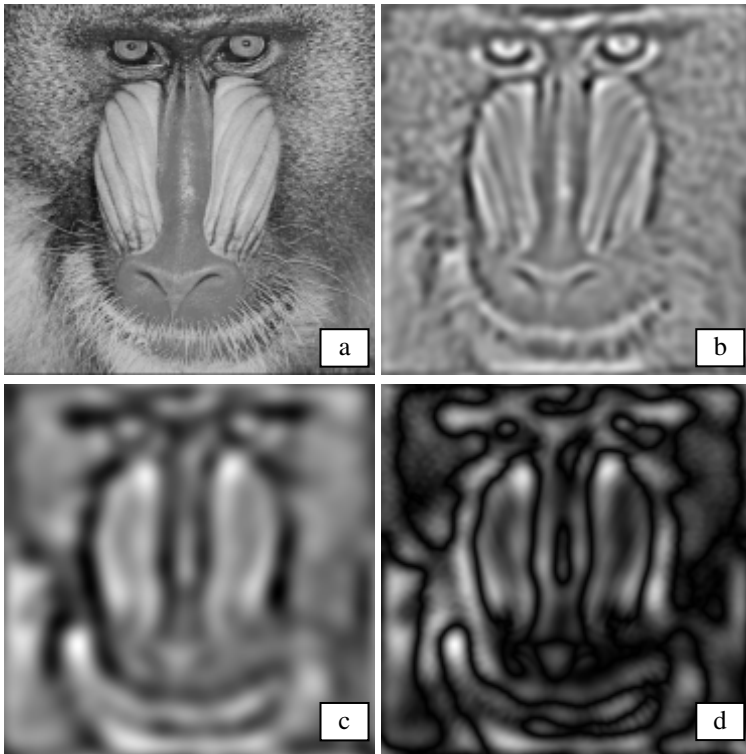


Fig. 2. (a) original image, (b) image filtered by Mexican Hat wavelet scale 3.0, (c) image filtered by Mexican Hat wavelet scale 4.0, and (d) scale interaction image between two different scales

After candidate points are found, the points that have a low contrast or are poorly localized are removed by measuring stability of each feature point at its location and scale. The stability of each feature point is calculated from a 2 by 2 Hessian matrix H as follows.

$$Stability = \frac{(D_{xx} + D_{yy})^2}{D_{xx}D_{yy} - D_{xy}^2} < \frac{(r+1)^2}{r}, \text{ where } H = \begin{bmatrix} D_{xx} & D_{xy} \\ D_{xy} & D_{yy} \end{bmatrix}. \quad (6)$$

r is the ratio between the largest and smallest eigenvalues and controls the stability. D represents image gradient of x - and y -axis.

Orientation of each feature point is assigned by considering local image properties. Orientation histogram is formed from gradient orientations at all sample points within the circular window of a feature point. Gradient magnitude m and orientation θ are computed by using pixel differences as follows.

$$m = \sqrt{(L_{x+1,y} - L_{x-1,y})^2 + (L_{x,y+1} - L_{x,y-1})^2}$$

$$\theta = \tan^{-1} \left(\frac{L_{x,y+1} - L_{x,y-1}}{L_{x+1,y} - L_{x-1,y}} \right) \tag{7}$$

L is a Gaussian filtered image with the closest scale, in which each feature point is found. Peak in this histogram corresponds to dominant direction of the feature point. Scale-invariant keypoints obtained through this process are invariant to rotation, scaling, translation, and illumination changes of images. Therefore, scale-invariant keypoints may be useful to design robust watermarking.

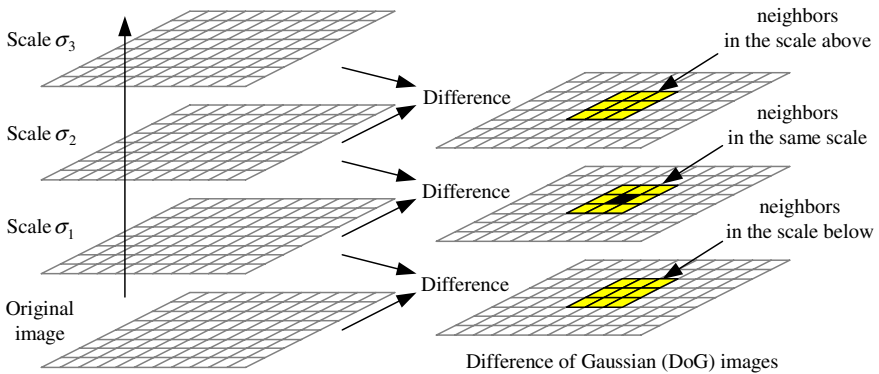


Fig. 3. Scale-space from the difference of gaussian function and the closest neighborhoods of a pixel.

3 Watermark Synchronization Using Feature Extraction

Watermarking algorithms are divided into two processes, watermark insertion and detection. Watermark insertion is a process of inserting the watermark into contents imperceptibly. Watermark detection is a process of detecting the inserted watermark from contents to prove ownership. General framework of feature-based watermarking is shown in Fig. 4 [8].

The first step for watermark insertion and detection is analyzing contents to extract features and then features are relatively related to generate the patches for watermarking. During watermark insertion, several patches are extracted from an image and the watermark is inserted into all patches. During watermark detection, there are several patches and all patches are tried to detect the watermark. We can prove ownership successfully if the watermark is detected correctly from at least one patch. Correlation-based detector is used to determine whether or not the watermark is inserted. Because the watermark is inserted multiple times into the image, it is highly likely that this method has high probability to detect the watermark even after attacks.

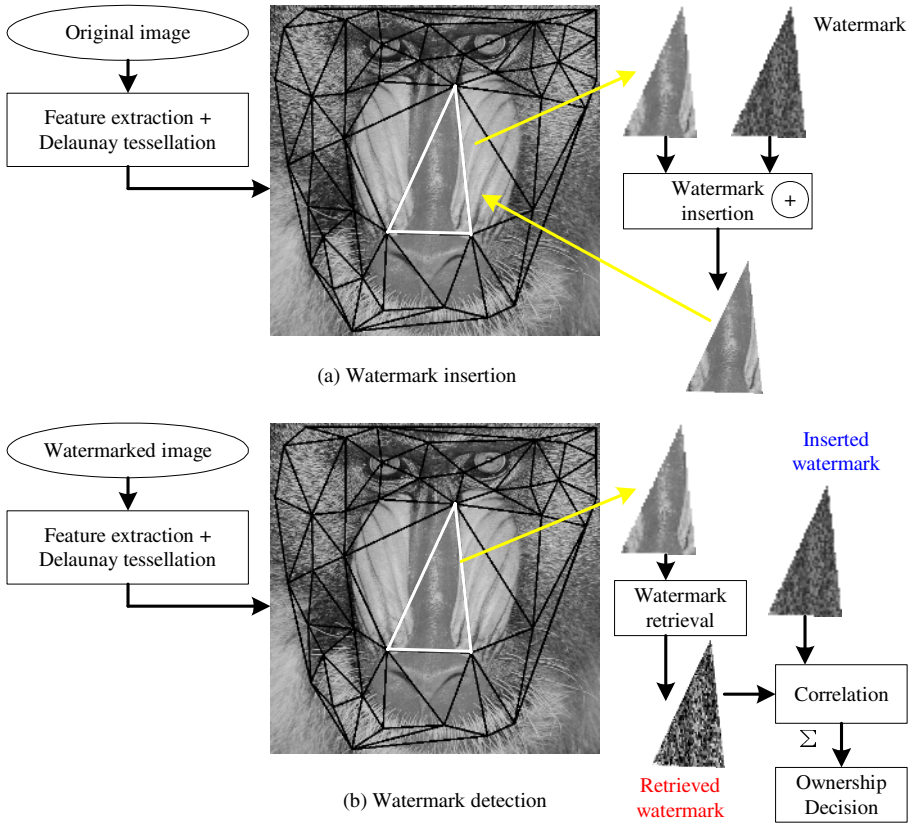


Fig. 4. Framework for watermark insertion and detection

As explained in Section 2, feature points are extracted by analyzing media contents. The feature points should be relatively related to generate the patches for watermark insertion and detection. Delaunay tessellation is commonly used to formulate the patches by decomposing the feature points into a set of disjoint triangles. Given a set of feature points, Delaunay tessellation is the straight line dual of the corresponding Voronoi diagram which partitions the image into segments such that all points in one segment are closer to the location of the feature points. This tessellation is independent of rotation, scaling, and translation of images. Moreover, computational cost is low. The extracted triangles are shaped irregularly. During watermarking, we require warping between the right-handed triangular watermark and the extracted triangles, which is affine transformation as follows.

$$\begin{pmatrix} x_n \\ y_n \end{pmatrix} = \begin{pmatrix} a_{11} & a_{12} \\ a_{21} & a_{22} \end{pmatrix} \begin{pmatrix} x_o \\ y_o \end{pmatrix} + \begin{pmatrix} s_1 \\ s_2 \end{pmatrix}. \tag{8}$$

(x_o, y_o) and (x_n, y_n) are coordinates of the original points and warped points respectively. This affine transformation is composed of 6 unknown parameters and mathematically calculated using three corner points of a triangle.

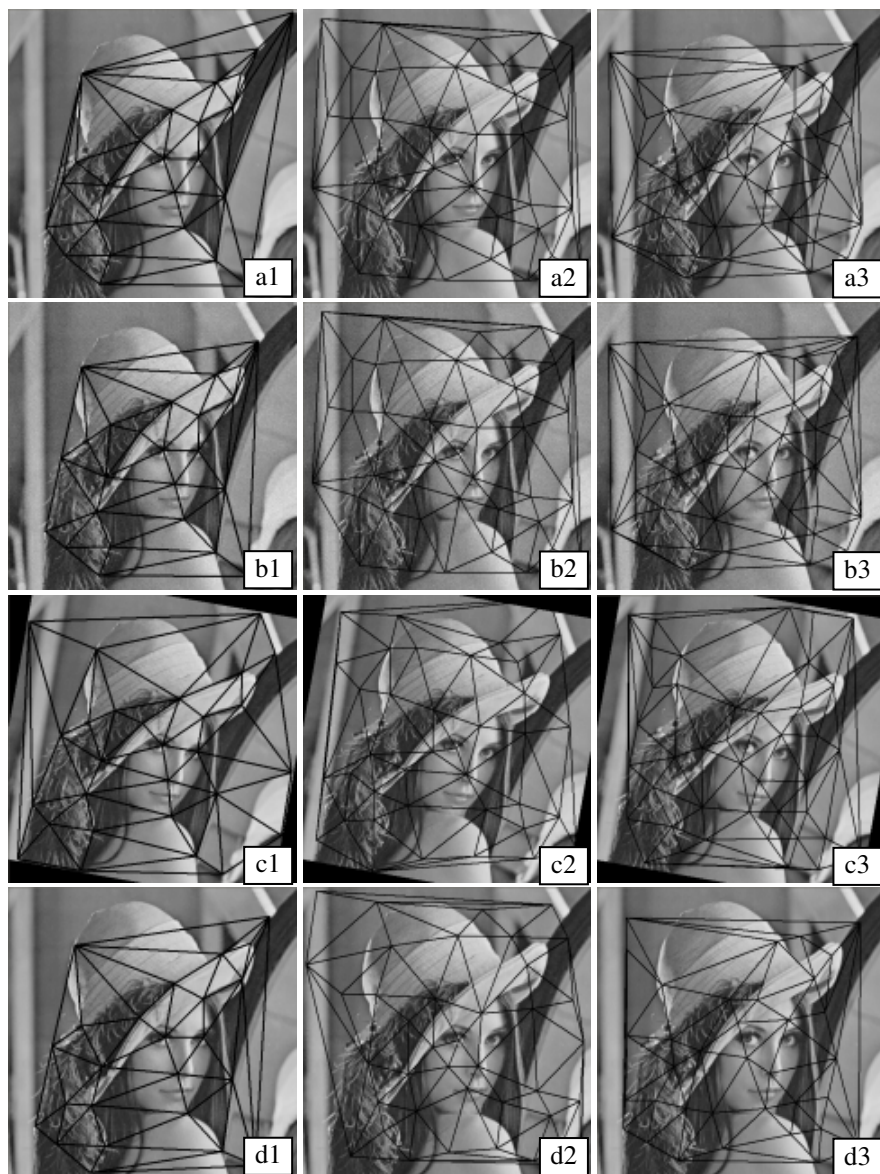


Fig. 5. Location for watermark insertion and detection against image attacks: (a) original image, (b) image with additive uniform noise, (c) image with rotation 10° , and (d) image with scaling 1.1x

As described in Bas *et al.* [8], the distribution of feature points is an important factor to design robust watermarking. In other words, the distance between adjacent feature points should be selected carefully. If the distance is too short, the distribution of the feature points is concentrated on textured areas. Furthermore, the size of the

patch for watermark insertion is too small to insert the watermark efficiently because the watermark should be sampled. If the distance is too long, feature points become isolated. In order to obtain the homogeneous distribution of feature points, we apply a circular neighborhood constraint, in which the feature points whose strength is the largest are selected [8]. The neighborhood size D is dependent on image dimension and quantized by r as follows.

$$D = \frac{w + h}{r}. \quad (9)$$

w and h represent the width and height of images, respectively. r is a constant to control the size. Circle diameter depends on image dimensions to be against scale change of images.

For feature extraction methods described in Section 2, Fig. 5 shows the extracted patches for watermarking against additive uniform noise, rotation 10° , and scaling 1.1x. The first column is from the Harris corner detector. The second column is from the Mexican Hat wavelet scale interaction method. The last column is from the scale-invariant keypoint extractor. Although signal processing attacks and geometric distortion attacks result in different tessellation by modifying relative position of the feature points, there are several corresponding patches. Therefore, we can synchronize successfully the location for watermark insertion and detection.

4 Evaluation Results

This section evaluates three feature extraction methods for robust watermarking: the Harris corner detector (method 1), the Mexican Hat wavelet scale interaction method (method 2), and the scale-invariant keypoint extractor (method 3).

We have used 15 images with the size of 512 by 512 pixels including commonly used images in image processing applications (see Fig. 6). Because our research focuses on watermarking of remote-sensing imagery, we include satellite images such as IKONOS (1.1m resolutions), SPOT (10m resolutions), and KOMPSAT (6.6m resolutions). Differently from natural images, satellite images contain much noise, similar patterns are repeated multiple times and that make feature extraction to be difficult. The quantization parameter r of the neighborhood size is set as 24, i.e. the minimum distance between adjacent feature points is about 42 pixels. The patches from this parameter may be small to watermark efficiently. On future works, we are going to adjust this parameter during applying watermarking scheme to the patches.

We applied signal processing attacks (median filter, Gaussian filter, additive uniform noise, and JPEG compression) and geometric distortion attacks (rotation, scaling, and cropping) listed in Stirmark 3.1.

For each method, the number of extracted patches is shown in Table 1. The averaged number from method 1, method 2, and method 3 were 73 patches, 79 patches, and 71 patches, respectively.

We measured redetection ratio of the patches, which represents how many patches that have been detected in the original image are correctly redetected in the attacked images. If the difference between the patches from the original image and the patches

from attacked images was less than two pixels, we regarded the patches as having been correctly redetected. These small misalignments can be compensated by searching some pixels around position of the patches originally founded during watermark detection. In particular, prior to comparison, we reversed coordinates of the patches in attacked images into coordinates in the original image by calculating their inverse transform.

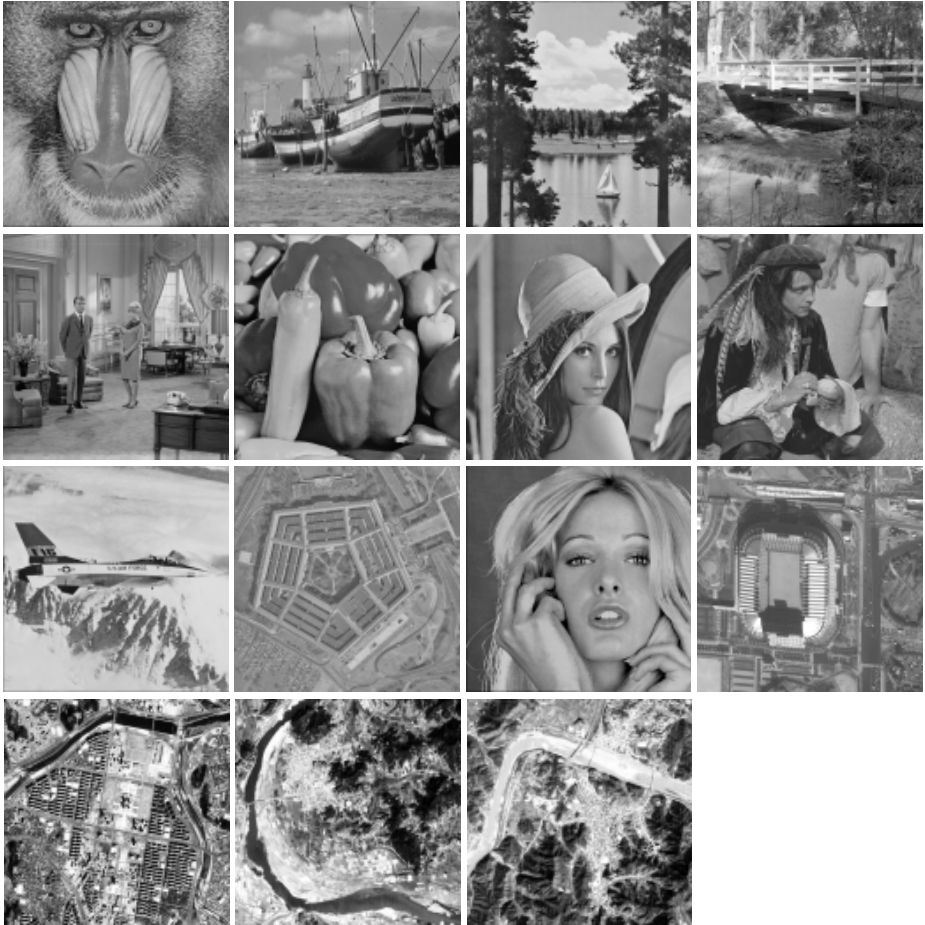


Fig. 6. Test images: Baboon, Boat, Lake, Bridge, Couple, Pepper, Lena, Indian, Plane, Pentagon, Girl, IKONOS, KOMPSAT, SPOT1, and SPOT2

Table 1. Number of extracted patches for each method

	Babo.	Boat	Lake	Brid.	Coup.	Pepp.	Lena	Indian	Plane	Penta.	Girl	Ikono.	Kom.	Spot1	Spot2
Method1	67	63	86	89	58	61	40	60	53	60	41	81	114	113	102
Method2	60	73	86	79	71	72	67	77	71	106	66	90	98	80	87
Method3	57	46	65	69	56	71	65	77	56	55	51	81	122	91	97

Table 2. Redetection ratios under signal processing attacks (unit %)

		Baboon	Lake	Bridge	Lena	Indian	Plane	Penta.	Ikonos	Komp.	Spot2	Total
Median 2×2	Method1	25	35	25	58	28	47	35	20	21	50	34
	Method2	50	57	76	85	88	77	56	82	68	78	73
	Method3	40	51	39	46	21	45	36	36	24	48	41
Median 3×3	Method1	39	33	28	55	35	17	28	25	13	52	35
	Method2	50	64	67	66	64	77	53	70	54	90	66
	Method3	19	17	36	29	27	55	36	17	37	32	34
Median 4×4	Method1	19	22	11	40	42	21	20	9	11	35	25
	Method2	23	41	52	67	48	24	47	29	23	82	48
	Method3	21	22	35	29	45	50	24	32	15	36	31
Gaussian filter	Method1	57	42	34	53	67	43	25	33	38	45	44
	Method2	90	77	92	85	78	90	64	84	92	90	85
	Method3	75	62	59	74	51	86	58	54	52	62	64
Uniform noise	Method1	45	38	30	58	25	28	27	23	35	43	41
	Method2	72	78	81	75	75	79	71	78	86	91	81
	Method3	42	62	51	72	44	59	29	52	57	47	53
JPEG comp. 40	Method1	67	36	37	58	47	38	27	21	40	45	46
	Method2	85	81	90	88	84	100	68	88	87	93	87
	Method3	60	80	59	57	35	89	64	58	53	61	61
JPEG comp. 50	Method1	48	47	37	60	37	32	37	32	41	56	46
	Method2	87	85	81	69	88	100	82	89	91	93	87
	Method3	72	57	51	77	64	88	55	62	62	81	65
JPEG com. 60	Method1	46	36	39	60	48	30	57	25	52	51	46
	Method2	85	78	95	90	74	97	81	97	87	93	89
	Method3	65	63	59	65	53	82	47	67	62	70	62
JPEG comp. 70	Method1	45	42	38	58	45	47	37	27	39	55	45
	Method2	97	81	91	88	87	100	78	89	91	93	90
	Method3	74	63	59	52	58	86	56	54	63	78	64
JPEG comp. 80	Method1	46	36	42	58	48	38	40	33	47	51	47
	Method2	92	78	97	94	77	100	84	82	90	93	90
	Method3	70	71	61	69	49	93	53	53	67	76	67
JPEG comp. 90	Method1	52	38	43	60	48	43	40	31	46	48	47
	Method2	98	78	95	90	77	100	81	92	90	93	90
	Method3	74	72	61	72	58	82	58	54	57	79	67

Table 2 shows redetection ratios under signal processing attacks and Table 3 shows redetection ratios under geometric distortion attacks. We represent results of several images. The last column represents the averaged detection ratios of 15 images.

Against signal processing attacks, method 2 based on the Mexican Hat wavelet scale interaction method outperformed than other methods. Because the Mexican Hat wavelet considers image intensity distributed to the wide area, small distortions in intensity do not affect performance. Because the Harris corner detector uses image gradients that are sensitive to image noise, method 1 based on the Harris corner detector showed relatively low performance and worked poorly in images which included complex texture like Baboon or contained much noise like satellite images: IKONOS and KOMPSAT. Method 3 using scale-invariant keypoints showed higher performance than method 1, but relatively lower performance than method 2.

Table 3. Redetection ratios under geometric distortion attacks (unit %)

		Baboon	Lake	Bridge	Lena	Indian	Plane	Penta.	Ikonos	Komp.	Spot2	Total
Crop 5%	Method1	34	27	30	40	25	34	40	10	26	28	30
	Method2	18	22	25	31	23	21	19	24	27	24	25
	Method3	25	38	42	42	23	63	38	27	39	51	38
Crop 10%	Method1	21	24	26	38	25	28	42	7	25	27	26
	Method2	15	16	23	18	22	13	15	11	14	22	18
	Method3	25	34	28	42	27	48	36	21	33	36	31
Crop 15%	Method1	22	23	18	38	28	23	38	4	19	25	24
	Method2	7	15	19	15	14	7	13	8	13	17	14
	Method3	19	28	20	26	17	43	25	14	32	30	25
Crop 20%	Method1	13	20	12	40	22	17	37	5	20	24	21
	Method2	5	5	11	7	16	3	8	4	11	15	9
	Method3	16	23	19	18	13	39	25	9	23	23	21
Crop 25%	Method1	9	16	11	38	18	15	32	1	18	23	18
	Method2	3	5	5	6	12	3	6	6	7	9	6
	Method3	9	18	17	15	13	29	20	10	20	21	17
Rotation 0.5° +Cropping	Method1	52	26	36	40	38	40	35	23	27	40	37
	Method2	80	53	58	55	52	48	47	48	58	70	57
	Method3	40	58	39	63	38	54	40	54	40	48	45
Rotation 1.0° +Cropping	Method1	31	21	28	40	32	34	23	25	18	35	32
	Method2	52	50	56	52	40	44	44	43	54	59	50
	Method3	47	38	38	42	38	61	44	51	33	44	42
Rotation 5.0° +Cropping	Method1	34	16	15	40	33	40	25	12	18	32	29
	Method2	27	33	34	39	39	23	26	29	44	40	33
	Method3	32	26	35	46	25	36	35	32	25	35	32
Rotation 10.0° +Cropping	Method1	33	21	27	33	27	26	22	11	19	22	25
	Method2	23	22	25	36	34	25	23	26	21	34	27
	Method3	21	23	35	38	21	45	47	41	25	33	33
Rotation 15.0° +Cropping	Method1	27	24	20	45	32	30	15	12	12	32	26
	Method2	17	24	30	36	23	17	21	24	22	30	25
	Method3	23	29	29	42	19	36	27	40	15	33	29
Rotation 30.0° +Cropping	Method1	25	17	19	40	23	30	25	14	12	34	24
	Method2	17	15	22	28	25	17	23	24	24	26	23
	Method3	26	18	17	23	18	21	29	33	16	25	23
Scaling 0.8×	Method1	10	10	6	20	3	15	42	11	4	19	19
	Method2	0	0	0	0	0	0	2	0	0	0	0
	Method3	11	9	13	8	8	11	13	12	7	8	10
Scaling 0.9×	Method1	33	20	18	23	40	34	35	22	6	37	29
	Method2	0	0	0	1	1	0	8	0	1	0	1
	Method3	19	22	30	12	5	11	35	23	11	21	19
Scaling 1.1× +Cropping	Method1	27	15	30	45	25	43	32	19	11	36	27
	Method2	5	0	13	4	1	3	24	0	4	6	5
	Method3	25	9	26	38	12	29	29	16	7	22	20
Scaling 1.2× +Cropping	Method1	12	15	13	43	22	30	17	4	5	25	20
	Method2	0	0	4	0	0	0	5	0	2	0	1
	Method3	11	11	7	15	5	11	13	4	5	7	8

Against most geometric distortion attacks except scaling attacks, method 3 performed relatively well. However, the performance differences were small to be ignorable. Method 1 worked better than other methods in scaling attacks because image gradients were preserved in scale change of images. Method 2 showed severe weak-

ness in scaling attacks. In scale changes of images, the response of the Mexican Hat wavelet is different, feature points are extracted in different position, and hence method 2 failed to redetect the patches. Method 3 showed relatively lower performance than method 1 in scaling attacks. However, overall performance is acceptable for watermarking purposes. We can prove the ownership if the watermark is detected from at least one patch.

5 Conclusion and Future Works

Watermark synchronization is crucial to design robust watermarking. One solution to find the location for watermark insertion and detection is by reference to image features. In feature-based watermarking, feature extraction is important to design robust watermarking, so feature extraction method should be selected carefully. This paper reviewed major feature extraction techniques: the Harris corner detector and the Mexican Hat wavelet scale interaction method. We evaluated the scale-invariant keypoint extractor in comparison with other techniques in aspect of watermarking. First, we extracted feature points. Then, the feature points were decomposed into a set of triangles by Delaunay tessellation. We measured the redetection ratio of the patches against geometric distortion attacks as well as signal processing attacks. The scale-invariant keypoint extractor showed acceptable performance for robust watermarking. Nevertheless, the redetection ratio in scaling attacks was relatively low. Our future research focuses on increasing robustness against geometric distortion attacks and applying the watermarking scheme to the patches.

References

1. M. Kutter: Watermarking resisting to translation, rotation and scaling. Proc. of SPIE, Vol. 3528 (1998) 423-431
2. S. Pereira, T. Pun: Robust template matching for affine resistant image watermark. IEEE Trans. on Image Processing, Vol. 9 (2000) 1123-1129
3. J.J.K.O. Ruanaidh, T. Pun: Rotation, scale and translation invariant spread spectrum digital image watermarking, Signal Processing, Vol. 66 (1998) 303-317
4. C. Lin, I.J. Cox: Rotation, scale and translation resilient watermarking for images. IEEE Trans. on Image Processing, Vol. 10 (2001) 767-782
5. D. Simitopoulos, D.E. Koutsonanos, M.G. Strintzis: Robust image watermarking based on generalized radon transformation, IEEE Trans. on Circuits and Systems for Video Technology, Vol. 13 (2003) 732-745
6. M. Arghoniemy, A.H. Twefik: Geometric invariance in image watermarking. IEEE Trans. on Image Processing, Vol. 13 (2004) 145-153
7. M. Kutter, S.K. Bhattacharjee, T. Ebrahimi: Towards second generation watermarking schemes. Proc. of ICIP, Vol. 1, (1999) 320-323
8. P. Bas, J-M. Chassery, B. Macq: Geometrically invariant watermarking using feature points. IEEE Trans. on Image Processing, Vol. 11 (2002) 1014-1028
9. A. Nikolaidis, I. Pitas: Region-based image watermarking. IEEE Trans. on Image Processing, Vol. 10 (2001) 1726-1740

10. C.W. Tang, H-M. Hang: A feature-based robust digital image watermarking scheme. *IEEE Trans. on Signal Processing*, Vol. 51 (2003) 950-959
11. B.S. Manjunath, C. Shekhar, R. Chellappa: A new approach to image feature detection with applications, *Pattern Recognition*, Vol. 4 (1996) 627-640
12. D.G. Lowe: Distinctive image features from scale-invariant keypoints. *International Journal of Computer Vision*, Vol. 60 (2004) 91-110
13. K. Mikolajczyk, C. Schmid: Scale and affine invariant interest point detectors. *International Journal of Computer Vision*, Vol. 60 (2004) 63-86
14. T. Tuytelaars, L.V. Gool: Matching widely separated views based on affine invariant regions. *International Journal of Computer Vision*, Vol. 59 (2004) 61-85